Cluster-Substrate Interaction on a Femtosecond Time Scale Revealed by a High-Resolution Photoemission Study of the Fermi-Level Onset

H. Hövel,* B. Grimm, M. Pollmann, and B. Reihl
University of Dortmund, Experimentelle Physik I, D-44221 Dortmund, Germany

(Received 24 July 1998)

We have measured ultraviolet photoemission spectra of quasi-size-selected silver clusters at $T = 40$ K grown in the nanopits of a graphite surface. The Fermi-level onset observed shows distinct deviations from the steplike shape typical for metals. A simple model that takes into account the finite lifetime of the photohole (corresponding to a charged cluster) can explain these deviations by the cluster-substrate interaction on a femtosecond time scale, and hence provide an explanation for the differences between photoemission spectra of free and deposited clusters in general. [S0031-9007(98)07729-1]

PACS numbers: 36.40.Mr, 61.16.Ch, 73.23.Ps, 79.60.–i

The electron energy measured in a photoemission experiment is influenced by the interaction with the remaining positive charge. In general, this is a dynamic process on a femtosecond time scale. An adiabatic and a sudden regime have been distinguished [1–3]. In the sudden limit, the photoelectron leaves so fast that the ionized system remains in the excited state until the photoelectron has left the region of interaction. In the other limit, the system evolves adiabatically in time. In that case the ejected electron picks up the relaxation energy, while this is missing in the sudden limit, giving rise to satellite structures or asymmetric line shapes [3]. For most photoemission experiments the sudden approximation was used for interpretation, but there are some examples of molecule or solid state spectroscopy where a *breakdown of the sudden approximation* was stated or a *transition from adiabatic to the sudden regime* was observed [4]. It was suspected [1] that these dynamic effects could be different for finite systems, like, e.g., clusters. Finally, in low dimensional samples the localized positive charge has been discussed as one possible effect responsible for unusual spectral shapes in photoemission [5], in particular, near the Fermi level.

In the past, photoelectron spectroscopy was used to study the electronic properties of free clusters in vacuum [6], and of clusters supported on substrates [7–10]. The importance of the remaining positive charge was studied for free clusters [11] but also stated in the case of clusters on substrates [12]. The influence of the substrate was discussed [9] in view of initial- and final-state effects on core-electron binding energies, and it was argued that dynamic effects should be visible for the intermediate cluster-substrate interaction on a graphite substrate, similar to a model yielding core level line shapes of adsorbates on a substrate [13]. However, these effects could not be identified because of limited energy resolution and nonuniform cluster size.

Here we present experimental ultraviolet photoemission spectroscopy (UPS) of the Fermi-level onset of quasi-size-selected silver clusters deposited on a graphite substrate. The use of a high energy resolution at low temperatures together with a method for controlled cluster growth in ultrahigh vacuum (UHV) revealed new features in the spectra, which can be described with a model considering the remaining positive charge on the cluster including the cluster-substrate interaction. Our results show that in these experiments neither the sudden nor the adiabatic approximation is applicable, but that dynamic effects on a femtosecond time scale determine the spectral shape of the Fermi-level onset. Femtosecond dynamics have been well known for cluster-substrate interactions [14]. Our observations fit well into the increasing interest in clusters on substrates, after many years of successful work on free clusters in vacuum.

The experiments were carried out in the surface-science facility described elsewhere [15]. It combines scanning tunneling microscopy (STM) at $T \leq 5$ K and high-resolution UPS ($\Delta E = 10$ meV) at $T \leq 50$ K. The silver clusters were produced by controlled condensation of metal evaporated onto a graphite (HOPG) surface with preformed pits of one monolayer depth and a diameter of 9 ± 2 nm [16]. Before the silver evaporation was performed in UHV, the nanostructured HOPG surface was heated 1 h at 870 K, and its cleanliness was checked by UPS. The size distribution of the clusters was determined by the combination of *in situ* UHV STM for the height and *ex situ* transmission electron microscopy (TEM) for the lateral diameter. The cluster-height distribution (cf. Fig. 1) as measured with STM was 2.4 ± 0.6 nm, 3.1 ± 0.7 nm, and 3.9 ± 0.8 nm. With a diameter-to-height ratio of 1.4 the mean number of atoms in the clusters are then $N = 9 \times 10^2$, 2×10^3, and 4×10^3, respectively.

The silver clusters produce a distinct signal in the spectra. By taking the difference curves of the spectra before and after silver evaporation, their spectral contribution could be extracted as described in Ref. [15]. By comparison of spectra for different silver coverages and cluster sizes we checked that this subtraction procedure completely removed the graphite signal. In Fig. 2 we

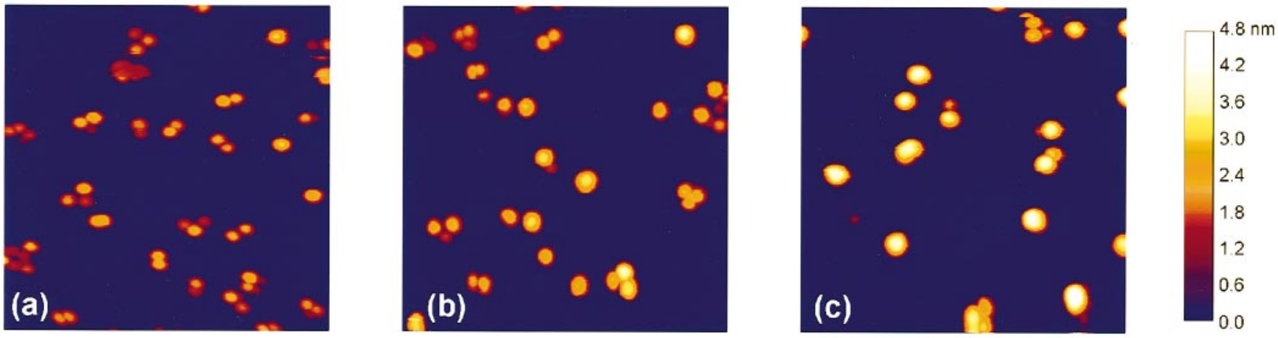

FIG. 1(color). Topographic STM images (scan area 150 × 150 nm^2) of silver clusters on graphite (HOPG) produced by controlled condensation in nanopits. Height distributions of (a) 2.4 ± 0.6 nm, (b) 3.1 ± 0.7 nm, and (c) 3.9 ± 0.8 nm; mean number of atoms in one cluster: 9×10^2, 2×10^3, and 4×10^3, respectively.

compare the spectra for the three different cluster sizes of Fig. 1 to the Fermi-level onset of bulk silver measured at $T = 40$ K. The bulk Fermi edge has a width of $\Delta E = 20$ meV defining the energy resolution with the pass energy of 2 eV used. All three spectra show similar features. At the Fermi energy there is a kink as sharp as the Fermi-level onset of bulk silver (see arrows in Fig. 2) followed by a nearly linear increase towards lower energies. The curves then level off to a constant signal with a smoothly rounded shape. This spectral shape becomes most evident for the largest clusters with $N = 4 \times 10^3$ atoms [cf. Fig. 2(c)] owing to the better statistics, but we present three typical spectra out of many (not shown). At first glance these spectra seem to indicate that the clusters are nonmetallic, because there is a vanishing density of states at the Fermi energy, which, however, is impossible for such large clusters and inconsistent with the pronounced plasmon resonance at approximately 3.5 eV which we observed (not shown) for all cluster sizes employing electron energy loss spectroscopy. The existence of a cluster plasmon proves the collective motion of the s electrons [17] typical for a metal.

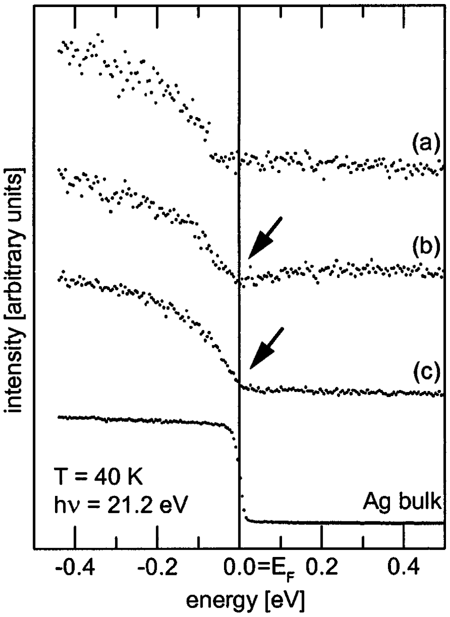

FIG. 2. The spectral contribution of the silver clusters in UPS, measured for the three different samples (a)–(c) of Fig. 1 at $T = 40$ K with $h\nu = 21.2$ eV. The bottom curve shows the Fermi-level onset of bulk silver measured with identical parameters. The arrows point to the characteristic kinks at the Fermi energy discussed in the text. The spectra are normalized to equal height of the Fermi-level onset.

Instead, we explain the observed spectral shape with a model which takes into account the influence of the photohole remaining on the metal cluster during the photoemission process and the cluster-substrate interaction. The charge remaining on the cluster after the photoionization process will cause a shift of the Fermi level. For a free cluster in vacuum, this energy shift describes roughly the difference between the ionization potential of the cluster and the work function of the bulk material. An exact calculation shows this shift is given by $\Delta E = \alpha e^2/4\pi\varepsilon_0 R$ with $\alpha = 0.41$ for silver clusters [11]. If one considers the cluster as a small particle of bulk, the contact with the substrate has to equalize the two Fermi energies. But this is valid only in a static view, since the charge transfer requires some time, depending on the strength of the cluster-surface interaction. For a cluster which is coupled to a substrate the energy shift is time dependent. It finally vanishes when an electron is regained from the substrate. For every single cluster this is a quantized process, since the charge amounts to $+e$. The measured energy of the photoelectron depends on how long the positive charge is remaining on the cluster. During this time interval there is an attractive force reducing the energy. Using a photon energy of 21.2 eV, an electron from the Fermi level is leaving the sample with a kinetic energy of about 17 eV, corresponding to a velocity of $\nu = 2.4 \times 10^6\ \mathrm{m\ s^{-1}}$ which is big enough to be sensitive to processes on a femtosecond time scale, because the electron travels a distance corresponding to several cluster radii (of the order of 10^{-9} m) during 10^{-15} s.

In a simple model, the elimination of the positive charge is described by a characteristic time τ which can be interpreted as a tunneling time in the case of a weak cluster-substrate interaction. τ will be dependent on the cluster radius, and, additionally, it can vary even for clusters of equal radius owing to a different cluster-substrate coupling. But as a first step we formulate our model for one cluster size and one time τ only. In a second step we will show that the results stay almost the same when we include the experimental cluster size distribution. The probability that the charge is eliminated during the time interval $[t, t + dt]$ is then given by

$$P(t)\,dt = (1/\tau)\exp(-t/\tau)\,dt\,. \tag{1}$$

In order to calculate the energy of the electron arriving at the electron energy analyzer, we need the potential $W(r)$ acting on the electron on its way from the cluster to infinity, with r being the distance from the center of the cluster. A simple formula which fits the limiting cases $W(R) = 0$ and $\lim_{r\to\infty}[\Delta E - W(r)] \propto 1/r$ and should give an estimation of the gross effects is given by

$$W(r) = \frac{\alpha e^2}{4\pi\varepsilon_0}\left(\frac{1}{R_{\text{cluster}}} - \frac{1}{r}\right). \tag{2}$$

If the charge on the cluster is neutralized after a time t, the energy shift for the electron is equal to $W(R + \nu t)$. The measured spectra average over a large number of photoelectrons with different times t. This leads—*even if all clusters are identical in radius and coupling to the substrate*—to a distribution of energy shifts given by $P(W)\,dW = P(t(W))(dt/dW)\,dW$ with $W \in [0, W_{\max}]$ and $W_{\max} = \Delta E$. The function $P(W)$ looks similar to the core level line shapes for adsorbates with different coupling strength to the substrate, studied theoretically [13] as well as experimentally [18]. If the clusters get very small, such a molecular model may also be applicable. The measured Fermi onset at low temperatures (where the thermal broadening is negligible) is formed by a superposition of sharp Fermi edges shifted with the distribution $P(W)$. With E_B being the binding energy this leads to $S(E_B) = \int_0^{W_{\max}} P(W)\Theta(E_B - W)\,dW$, with $\Theta(x) = 0$ for $x < 0$ and $\Theta(x) = 1$ for $x \geq 0$. Finally, with $C = (R/\nu\tau)$

$$S(E_B) = \begin{cases} 1 - \exp(-\frac{CE_B}{W_{\max} - E_B}), & \text{for } E_B < W_{\max}, \\ 1, & \text{for } E_B \geq W_{\max}\,. \end{cases} \tag{3}$$

The function $S(E_B)$ is plotted for several values of C in Fig. 3(a). For $C \ll 1$ the Fermi onsets are shifted by $W_{\max}$. This corresponds to the case of free clusters with an infinite lifetime of the photohole. For $C \gg 1$ we observe Fermi onsets at $E_B = 0$, because the photohole is immediately neutralized. In the intermediate range, we find curves with different curvatures, depending on the value of C.

To check on the influence of the cluster size distribution we assumed a Gaussian distribution with $R = \overline{R} \pm 0.2\overline{R}$, which corresponds to the measured cluster sizes [16]. Calculated $S(E_B)$ curves for the different values of C were summed up with varying $W_{\max}$ according to the size distribution. The results are shown in Fig. 3(b). It is remarkable that the curves for $C > 1$ are almost unchanged by the cluster size distribution. Especially the kink at the Fermi energy remains as sharp as for monodispersed clusters.

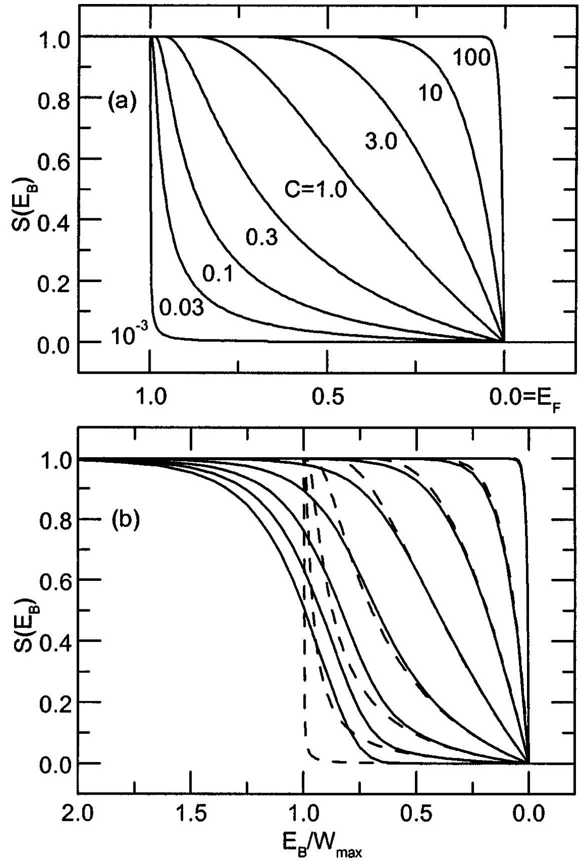

FIG. 3. (a) Photoemission spectra calculated with Eq. (3) for several values of $C = (R/\nu\tau)$ assuming clusters identical in radius and coupling to the substrate. (b) Comparison of spectra calculated assuming a Gaussian size distribution with $R = \overline{R} \pm 0.2\overline{R}$ (full lines) and the spectra of (a) (dashed lines).

In Fig. 4 we show that the experimental spectrum for the clusters with $N = 4 \times 10^3$ atoms at $T = 40$ K can be described by our model if we choose the parameters $C = 3.0$ and $W_{\max} = 0.49$ eV. Together with the mean cluster radius $\overline{R} = 2.5$ nm this results in $\tau = 0.3 \times 10^{-15}$ s which is of the expected order of magnitude for a coupling with significant cluster-substrate interaction as in the case of graphite. The value of $W_{\max} = 0.49$ eV is larger than $\Delta E = 0.24$ eV, the number given in Ref. [11] for free silver clusters of the same size. This may be an indication that the cluster-substrate interaction not only provides values $C > 0$, but also changes the total shift given by $W_{\max}$ (cf. Ref. [7]). We also show in Fig. 4 the cluster signal at the Fermi energy with the

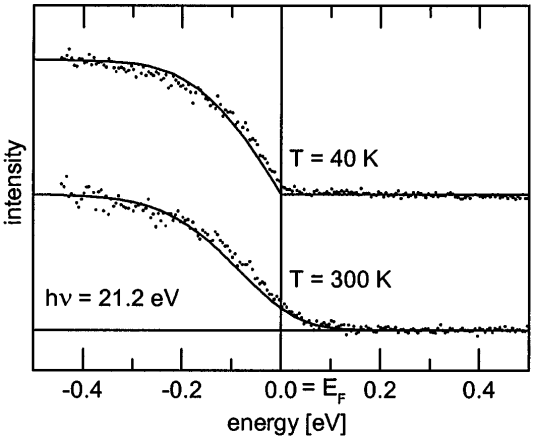

FIG. 4. Top curve: Comparison of the experimental spectrum measured at $T = 40$ K for clusters with 4×10^3 atoms and the spectra calculated using Eq. (3) with $C = 3.0$, $W_{\max} = 0.49$ eV, and $R = \overline{R} \pm 0.2\overline{R}$. Bottom curve: Experimental spectrum measured at $T = 300$ K, and calculated spectrum including thermal broadening, both of which do not reveal the characteristic kink at the Fermi energy.

measurements made at room temperature. In this case the thermal broadening of the Fermi edge masks the sharp kink at the Fermi energy, which is also evident in the calculated spectrum using identical parameters as at low temperatures, but convoluting a room temperature Fermi function. Therefore, performing UPS with high energy resolution at low temperatures was crucial for the clarification of the cluster-substrate interaction.

The shape of the spectra for smaller cluster sizes [cf. Fig. 2(a)] seems to indicate smaller values of C *without* the characteristic kink; however, our statistics is not good enough for a model fit. We also do not want to stress the quantitative agreement, because of the simplifications included in our model. For example, the nonspherical cluster shapes and screening effects due to the polarizibility of the substrate are not included and the simple potential given by Eq. (2) may need some refinement. But the model describes well the principal effects. Especially we want to point out the inherent quantum mechanical size effect which is included in the probability distribution (1). We rely on the fact that single photoemission processes are characterized by statistically distributed times t, otherwise we would get a shifted Fermi energy broadened by the cluster size distribution. But with the cluster sizes measured this cannot explain the spectra obtained, as we can see in Fig. 3(b) for $C \ll 1$. Instead of the sharp kink we would obtain a gap at the Fermi energy, which could clearly be observed with our experimental energy resolution.

We thank F. Katzenberg and Professor J. Petermann for taking the TEM pictures and G. Pike and F. Ströwer for their technical assistance with the experiments.

---

*Electronic addresses: hoevel@physik.uni-dortmund.de; http://el.physik.uni-dortmund.de

[1] J.W. Gadzuk and M. Šunjić, Phys. Rev. B **12**, 524 (1975).
[2] C. Noguera, D. Spanjaard, and J. Friedel, J. Phys. F **9**, 1189 (1979).
[3] S. Doniach and M. Šunjić, J. Phys. C **3**, 285 (1970).
[4] M. Bertolo, W. Hansen, P. Althainz, J. Schreiner, and K. Jacobi, Chem. Phys. Lett. **196**, 552 (1992); D.D. Samra, C. Carbone, P. Sen, R. Cimino, and W. Gudat, Phys. Rev. Lett. **63**, 656 (1989); F.J. Himpsel, D.E. Eastman, and E.E. Koch, Phys. Rev. Lett. **44**, 214 (1980).
[5] B. Dardel, D. Malterre, M. Grioni, P. Weibel, Y. Baer, and F. Lévy, Phys. Rev. Lett. **67**, 3144 (1991).
[6] O. Cheshnovsky, K.J. Taylor, J. Conceicao, and R.E. Smalley, Phys. Rev. Lett. **64**, 1785 (1990); G. Ganteför, K.H. Meiwes-Broer, and H.O. Lutz, Phys. Rev. A **37**, 2716 (1988).
[7] G.K. Wertheim, S.B. DiCenzo, and S.E. Youngquist, Phys. Rev. Lett. **51**, 2310 (1983).
[8] M.G. Mason, Phys. Rev. B **27**, 748 (1983); L. Oberli, R. Monot, H.J. Mathieu, D. Landolt, and J. Buttet, Surf. Sci. **106**, 301 (1981).
[9] S.L. Qiu, X. Pan, M. Strongin, and P.H. Citrin, Phys. Rev. B **36**, 1292 (1987).
[10] H.-J. Freund, Angew. Chem. Int. Ed. **36**, 452 (1997), and references therein.
[11] M. Seidl, K.-H. Meiwes-Broer, and M. Brack, J. Chem. Phys. **95**, 1295 (1991).
[12] G.K. Wertheim, S.B. DiCenzo, and D.N.E. Buchanan, Phys. Rev. B **33**, 5384 (1986).
[13] K. Schönhammer and O. Gunnarsson, Solid State Commun. **23**, 691 (1977).
[14] Bu. Wrenger, K.H. Meiwes-Broer, O. Speer, and M.E. Garcia, Phys. Rev. Lett. **79**, 2562 (1997); D. Steinmüller-Nethl, R.A. Höpfel, E. Gornik, A. Leitner, and F.R. Aussenegg, Phys. Rev. Lett. **68**, 389 (1992).
[15] H. Hövel, T. Becker, D. Funnemann, B. Grimm, C. Quitmann, and B. Reihl, J. Electron Spectrosc. Relat. Phenom. **88-91**, 1015 (1998).
[16] H. Hövel, Th. Becker, A. Bettac, B. Reihl, M. Tschudy, and E.J. Williams, J. Appl. Phys. **81**, 154 (1997).
[17] W.A. de Heer, K. Selby, V. Kresin, J. Masui, M. Vollmer, A. Châtelain, and W.D. Knight, Phys. Rev. Lett. **59**, 1805 (1987); U. Kreibig and M. Vollmer, *Optical Properties of Metal Clusters*, Springer Series in Materials Science Vol. 25 (Springer-Verlag, Berlin, Heidelberg, 1995).
[18] J.C. Fuggle, E. Umbach, D. Menzel, K. Wandelt, and C.R. Brundle, Solid State Commun. **27**, 65 (1978).